Drosophila Lis1 is required for neuroblast proliferation, dendritic elaboration and axonal transport

Zhao Liu*, Ruth Steward† and Liqun Luo*‡

**Department of Biological Sciences, Stanford University, Stanford, California 94305-5020, USA*
†The Waksman Institute, Department of Molecular Biology and Biochemistry, Rutgers University, Piscataway, New Jersey 08854, USA
‡e-mail: lluo@stanford.edu

Haplo-insufficiency of human *Lis1* causes lissencephaly. Reduced Lis1 activity in both humans and mice results in a neuronal migration defect. Here we show that *Drosophila Lis1* is highly expressed in the nervous system. *Lis1* is essential for neuroblast proliferation and axonal transport, as shown by a mosaic analysis using a *Lis1* null mutation. Moreover, it is cell-autonomously required for dendritic growth, branching and maturation. Analogous mosaic analysis shows that neurons containing a mutated cytoplasmic-dynein heavy chain (*Dhc64C*) exhibit phenotypes similar to *Lis1* mutants. These results implicate Lis1 as a regulator of the microtubule cytoskeleton and show that it is important for diverse physiological functions in the nervous system.

The most common cause of classical lissencephaly, or 'smooth brain', is the inactivation of one copy of the human *Lis1* gene[1,2]. Reduced levels of Lis1 activity in both humans and mice results in a defect in neuronal migration[1,3]. However, careful analysis of heterozygous *Lis1* mice has revealed abnormalities that are distinct from those seen in mice harbouring mutations in other neuronal-migration genes[3], indicating that *Lis1* may have further functions in the developing nervous system. The complete loss-of-function phenotype of *Lis1* mutations in neurons has not been described, as mice that are homozygous-null for *Lis1* die as early embryos before formation of the nervous system.

Lis1 protein is highly conserved from humans[2] to *Drosophila*[4,5] and *Aspergillus*[6], and is composed of an amino-terminal coiled-coil domain and seven WD-40 repeats[7]. Biochemically, Lis1 has been identified as the non-catalytic subunit of platelet-activating factor (PAF) acetylhydrolase[8], which may modulate the activity of PAF. Lis1 may interact with microtubules and reduce microtubule catastrophe events[9]. The Lis1 homologue in *Aspergillus*, *nudF*, was

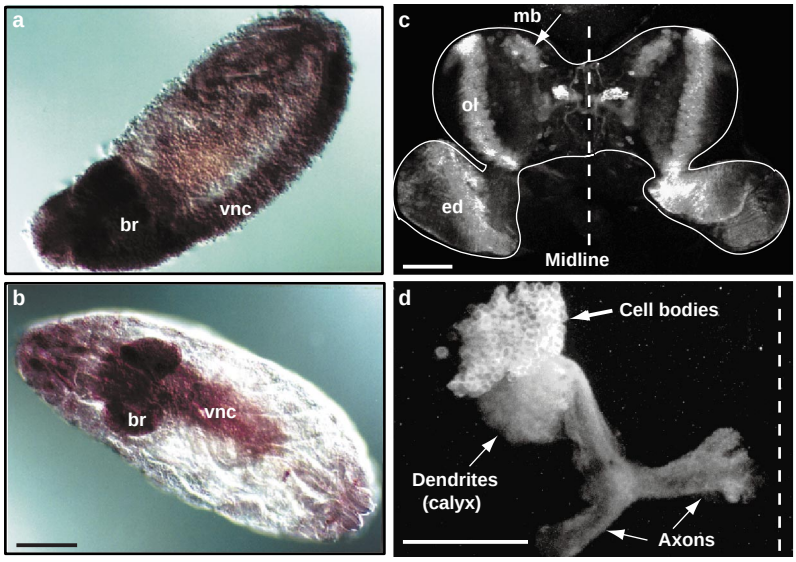

Figure 1 ***Lis1* is strongly expressed in the CNS and is distributed throughout mushroom-body neurons. a**, **b**, *In situ* hybridization of *Lis1* in wild-type embryos, showing that *Lis1* transcripts highly enriched in the brain (br) and the ventral nerve cord (vnc) at stages 13 (**a**) and 16 (**b**) of embryonic development. Scale bar represents 50 µm. **c**, **d**, Anti-HA immunofluorescence staining, illustrating the expression of HA-tagged Lis1 under the control of the GAL4^{OK107} promoter in eye discs (ed), optic lobes (ol) and mushroom bodies (mb; **c**). HA–Lis1 is distributed throughout the cell bodies, dendrites, and axonal lobes of mushroom-body clones (**d**). Dashed lines indicate the midline. Scale bars represent 50 µm. Genotypes are as follows: **c**, *UAS–HA–Lis1/+; GAL4^{OK107}/+*. **d**, *hs–FLP, UAS–mCD8–GFP/+; FRT^{G13}/ FRT^{G13}, tubP–GAL80; UAS–HA–Lis1/+; GAL4^{OK107}/+*.

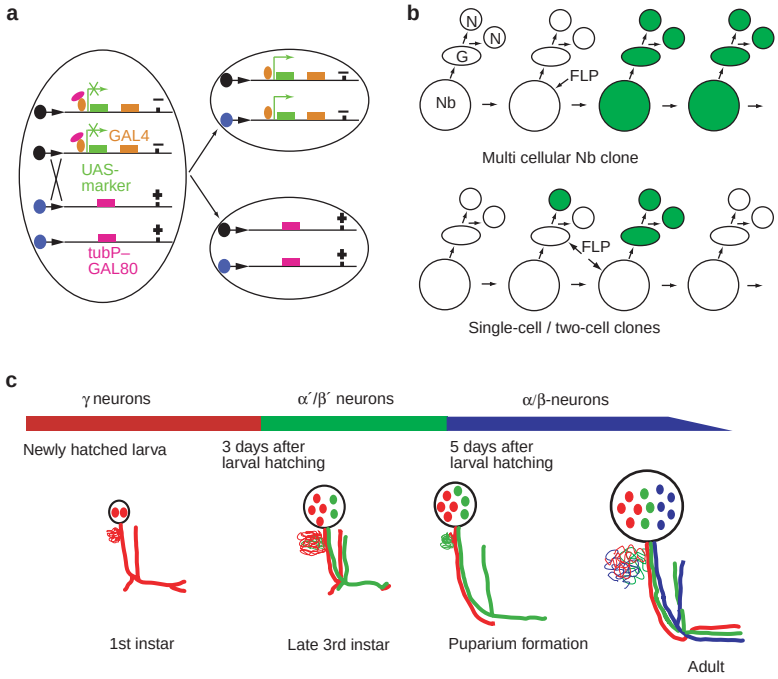

Figure 2 **Illustration of MARCM and mushroom-body development. a**, Schematic summary of mosaic analysis with a repressible cell marker (MARCM). The marker positively labels homozygous mutant (–) clones[13]. In the heterozygous parental cell, a GAL4-driven UAS-marker is not expressed, because of the presence of the repressor, GAL80. When FLP-mediated mitotic recombination occurs at the FRT sites (arrowheads), homozygous-mutant cells express the marker as a result of the loss of the GAL80 repressor. **b**, Schematic representation of the pattern of neuroblast proliferation in *Drosophila* and the three types of labelled clones visualized by MARCM. When FLP-mediated mitotic recombination occurs in a dividing neuroblast (Nb), a daughter neuroblast can be labelled as a result of loss of the repressor gene; all neurons generated in this lineage will be marked (neuroblast clone). Alternatively, a ganglion mother cell (G) could be labelled and thus a clone of two postmitotic neurons (N) can be generated (two-cell clone). If mitotic recombination occurs during a division of the ganglion mother cell, only one post-mitotic cell is labelled (single-cell clone). **c**, Summary of mushroom-body development[14]. Starting in the late embryo and continuing until adult hatching, each neuroblast sequentially generates three types of neurons with different patterns of axonal projection. During metamorphosis at the early pupal stage, γ-neurons (red) undergo extensive reorganization of dendrites and axons. Therefore, when early born γ-neurons are examined in the adult, their dendrites and most of the axons are essentially products of regeneration that has occurred during metamorphosis, about 5 days after induction of clones. The problem associated with protein perdurance is greatly reduced in these adult clones.

originally identified through the nuclear-migration phenotype of its mutants[6]. *nudF* shows strong genetic interaction with *nudA*, which encodes a cytoplasmic-dynein heavy chain[10], and with α-tubulin in *Aspergillus*[11], indicating that Lis1 may be closely associated with the microtubule cytoskeleton. Genetic analysis of *Lis1* function in *Drosophila* oogenesis has shown that *Lis1*, similar to *Dhc64C*, is essential for germline-cell division[4], nuclear positioning[5], and oocyte differentiation[4,5], which supports the idea that Lis1 functions with the dynein complex and the microtubule cytoskeleton.

To examine the functions of *Lis1* in neurons *in vivo*, we carried out a genetic mosaic analysis of *Lis1* in the developing *Drosophila* brain. We identified essential functions of Lis1 in neuroblast proliferation, dendritic growth and branching, as well as a probable function in axonal transport. Interestingly, an analogous mosaic analysis showed that neurons containing a mutated cytoplasmic-dynein heavy chain exhibit phenotypes similar to *Lis1* mutants. These findings support a model in which Lis1 regulates the microtubule cytoskeleton, and reveal the diverse physiological functions of Lis1 in the nervous system.

Results

***Drosophila* Lis1 is highly enriched in the nervous system.** *Drosophila Lis1* has been shown to be highly expressed in oocytes, where it carries out essential functions[4,5]. High levels of *Lis1* RNA are uniformly distributed in early embryos, presumably as a result of maternal contribution[4]. Coincident with the onset of neuronal differentiation at embryonic stage 13, *Lis1* transcript becomes highly enriched in the developing central nervous system (CNS; Fig. 1a). At later stages of embryogenesis, while expression in other tissues decreases, high levels of *Lis1* RNA persist in the nervous system (Fig. 1b). *Lis1* is also highly expressed in third-instar larval brain and imaginal discs (data not shown).

To gain insight into the function of *Lis1*, we determined its subcellular distribution in the CNS by creating a transgene encoding Lis1 tagged with a haemagglutinin (HA) epitope, expressed under the control of the GAL4–UAS system[12]. To examine the distribution of HA–Lis1 in mushroom-body neurons, the 'model' neuron used for most of this study, we either crossed *UAS–HA–Lis1* directly to neuronal GAL4 drivers, or generated MARCM (mosaic analysis with a repressible cell marker) clones, such that the transgene would only be expressed in a small subset of clonally derived neurons (Fig. 2; ref. 13). These approaches avoided detection of widespread expression of Lis1 in the complex CNS and thus gave increased resolution. In both cases, we found HA–Lis1 to be distributed throughout cell bodies, dendrites and axons of the mushroom-body neurons (Fig. 1c, d).

Strategies to study *Lis1* function in the CNS. *Lis1* is essential for oogenesis, and homozygous *Lis1*-null mutants die as larvae, presumably because the requirement for *Lis1* in embryogenesis, including development of the nervous system, is met by the strong maternal

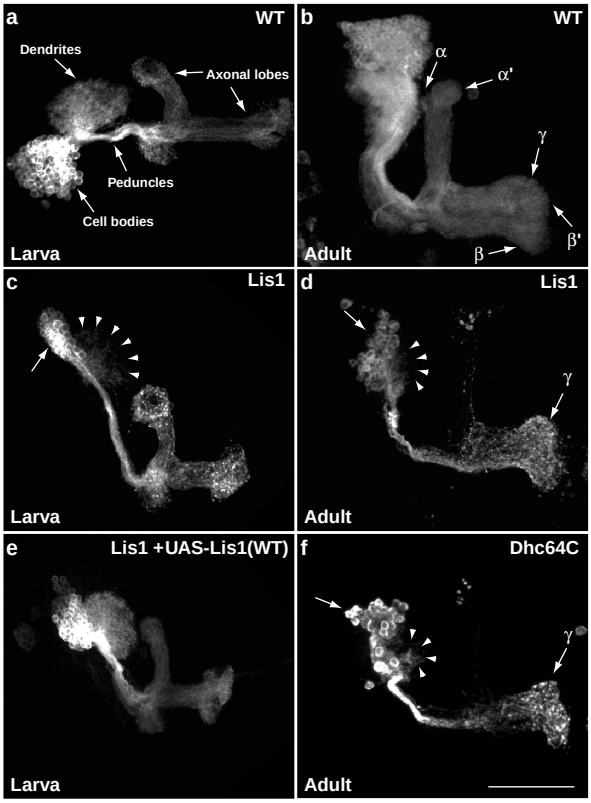

Figure 3 **Gross phenotypes of *Lis1* and *Dhc64C* in mushroom-body neuroblast clones. a**, **c**, At the late third-instar larval stage, a wild-type (WT) mushroom-body neuroblast clone (**a**) contains ~150 cells, well-extended dendrites, axonal peduncles and two axonal lobes. A *Lis1* neuroblast clone (**c**) has ~50 cells (arrow) with markedly reduced dendrites (arrowheads). A wild-type adult neuroblast clone (**b**) has ~500 cells and 5 axonal lobes. In contrast, *Lis1* adult clones (**d**) continue to have ~50 cells (arrow), sending their axons into the γ-lobe, with very few dorsal projections. The dendritic region is reduced (arrowheads). Note the axonal swellings, which are most severe in the lobe region (**c**, **d**). Expression of a *UAS–Lis1* (WT) transgene (**e**) completely rescues the *Lis1* phenotype. An adult mushroom-body clone of *Dhc64C* (**f**) shows striking similarities with that of *Lis1* (**d**), having a reduced neuronal number, weak dendrites, and axonal swellings. Images are composites of confocal sections; unless otherwise stated, signals are from anti-mCD8 immunostaining. Scale bar represents 50 μm. Genotypes are as follows: **a**, **b**, *hs–FLP, UAS–mCD8-GFP/X or Y; FRT^{G13}/ FRT^{G13}, tubP–GAL80; $GAL4^{0K107}$/+*. **c**, **d**, *hs–FLP, UAS–mCD8–GFP/X or Y; FRT^{G13}, $Lis1^{G10.14}$/ FRT^{G13}, tubP–GAL80; $GAL4^{0K107}$/+*. **e**, *hs–FLP, UAS–mCD8–GFP/X or Y; FRT^{G13}, $Lis1^{G10.14}$/ FRT^{G13}, tubP–GAL80; UAS–Lis1; $GAL4^{0K107}$/+*. **f**, *hs–FLP, UAS–mCD8–GFP/X or Y; FRT^{2A}, $Dhc64C^{4-19}$/FRT^{2A}, tubP–GAL80; $GAL4^{0K107}$/+*.

contribution[4]. We used the MARCM strategy[13] to create uniquely marked homozygous *Lis1* clones in otherwise heterozygous animals. In the MARCM strategy, a cell marker is under the control of a repressible promoter, and the repressor is driven by a ubiquitous promoter that prevents the expression of the marker in heterozygous cells. Thus, only in homozygous mutant cells will the marker be expressed (Fig. 2a). We focused primarily on the function of *Lis1* in developing neurons of the mushroom body, the insect centre for learning and memory. The development of wild-type mushroom-body neuronal projections from early larva to adulthood has been extensively studied at the single-cell level (ref. 14; Fig. 2c), thus aiding the analysis of *Lis1*-mutant phenotypes. For most of this study, we used a membrane-targeted protein tagged with green fluorescent protein, mCD8–GFP[13], to mark the entire axonal and dendritic projections of *Lis1*-mutant cells. The pattern of cell division in the *Drosophila* CNS predicts the generation of three types of clones — multicellular neuroblast clones, two-cell clones and single-cell clones (Fig. 2b) — in different mosaic animals, each of which can be used to analyse different aspects of *Lis1* function.

***Lis1* is essential for neuroblast proliferation.** A wild-type mushroom-body neuroblast clone (Fig. 2b) generated in 0–2-h-old larvae gave rise to ~200 mushroom-body neurons by the end of larval life (4.5 days later), with characteristic dendritic projections and axons through the peduncle into the dorsal and medial lobes (Fig. 3a). When examined in adults, a clone of >500 mushroom-body neurons, including 3 types of sequentially generated neurons, projected their axons into 5 distinct lobes (Fig. 3b, summarized in Fig. 2c; see also ref. 14). Mushroom-body neuroblast clones homozygous for a *Lis1*-null mutant, $Lis1^{G10.14}$ (used in this and all subsequent analysis; ref. 4), contained only ~50 neurons when examined both at the end of the larval life (Fig. 3c) and in adults (Fig. 3d). The reduction in clone size, as well as all other phenotypes described in this manuscript, were fully rescued by a wild-type *Lis1* transgene in larvae (Fig. 3e) and adults (data not shown), indicating that these defects are caused by the lack of *Lis1* activity.

Several lines of evidence indicate that the reduced *Lis1* clone size was caused by defects in cell birth, rather than cell death. First, clones examined at the end of larval life and in adults were of similar size. In fact, mushroom-body neuroblast clones from 2-week-old adults had no obvious reduction in neuronal numbers as compared with those examined in 1-day-old adults (data not shown), even though no mushroom-body neurons are born in adults[14]. Second, most neurons in *Lis1* neuroblast clones projected their axons only to the medial lobe in adults, indicating that they were γ-type mushroom-body neurons, which are the first among the three classes to be born[14] (Fig. 2c). Finally, to provide a direct demonstration of a neuroblast-proliferation defect, we carried out 5-bromodeoxyuridine (BrdU) pulse-labelling experiments (Fig. 4). We induced mushroom-body clones in newly hatched larvae, which we subsequently fed with BrdU for 3 h at defined stages to label proliferating cells. We dissected and fixed the brains at the end of larval life, for examination of mushroom-body neuroblast clones and BrdU incorporation. Wild-type mushroom-body neuroblast clones generated new neurons at all times examined (strong BrdU-labelled mushroom-body neurons in Fig. 4a, b; see also Fig. 4e). In contrast, *Lis1* mushroom-body neuroblast clones contained fewer BrdU-positive cells as development progressed (Fig. 4c–e), until neuroblast proliferation appeared to be arrested at roughly the mid-larval stage. The timing of this arrest is consistent with the presence of mainly γ-neurons and occasionally a few α′/β′ neurons in *Lis1* clones, as the transition between these two types of neuron occurs roughly three days after larval hatching[14]. The perdurance of mRNA or protein inherited from parental cells at the time of clone generation may explain why mutant neuroblasts can still proliferate for a few days before the final arrest. We examined *Lis1* neuroblast clones around the time of neuroblast-proliferation arrest, using anti-lamin antibody to visualize nuclear morphology[15] and propidium iodide to stain DNA. No obvious defects in nuclear morphology or ploidy were detected (data not shown). Together with the previous demonstration that *Lis1* is required for cell division in oogenesis[4], these results support a general function of Lis1 in cell division.

Cell-autonomous functions of *Lis1* in dendritic growth, branching and maturation. When we compared mushroom-body neuronal processes in wild-type and *Lis1* mushroom-body neuroblast clones at the end of larval life (Fig. 3a, c), one salient feature was that the fluorescence intensity of the dendritic fields of *Lis1* clones was much weaker than that of wild-type clones. Taking into consideration that *Lis1* clones are composed of fewer mushroom-body neurons, we quantified the extent of dendritic projections by dividing the total fluorescence intensity of the dendritic field by that of the cell bodies[15]. This quantification yielded a sixfold reduction in the ratio of dendritic to cell-body fluorescence in *Lis1* clones relative to the wild type (Fig. 5A, a). This quantitative difference is likely to be

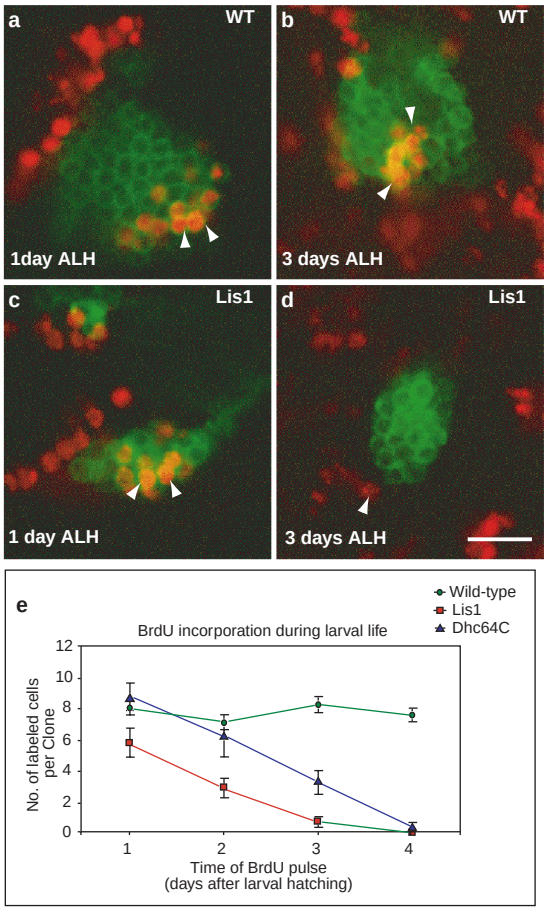

Figure 4 ***Lis1* and *Dhc64C* are required for proliferation of mushroom-body neuroblasts.** Mitotic recombination was induced at 0–2 h after larval hatching (ALH); BrdU pulse labelling was carried out at 1, 2, 3, or 4 days ALH. **a–d**, Single confocal sections taken from the brains of wandering third-instar larvae. GFP signal (green) shows clonal cells, and staining with anti-BrdU antibody (red) indicates cells that incorporated BrdU during the pulse-labelling period. At 1 day ALH, both wild-type (WT, **a**) and *Lis1* (**c**) clones incorporate BrdU into the proliferating neurons (arrowheads). At 3 days ALH, unlike wild-type clones (**b**), *Lis1* clones (**d**) lose the ability to incorporate BrdU. Note that the neighbouring wild-type mushroom-body neuroblasts still incorporate BrdU (**d**, arrowhead). Scale bar represents 10 μm. **e**, Graph showing the progressive reduction in the rate of BrdU incorporation into *Lis1* and *Dhc64C* mushroom-body neuroblast clones. Values are means ± s.e.m.; n = 6–20. Genotypes of wild-type, *Lis1* and *Dhc64C* clones are as described in Fig. 3b, d and f, respectively.

an underestimate, as early born mushroom-body neurons tend to have more elaborate dendrites[14]. These observations indicate that Lis1-mutant mushroom-body neurons have a severe reduction in overall dendritic projection.

To determine the nature of the dendritic defect and to determine whether Lis1 functions in a strictly cell-autonomous manner in regulating dendritic development, we analysed mosaic animals in which only single mushroom-body neurons were homozygous for *Lis1* (Fig. 2b). We generated these single-cell clones in newly hatched larvae. When we analysed them at the end of larval life, no obvious difference was apparent between wild-type and *Lis1* clones (Fig. 5A, b and c), despite the fact that strong overall defects were seen in *Lis1* neuroblast clones (compare Figs 3a, c and 5A, a). This is probably a result of the perdurance of Lis1 protein in single-cell clones. The defects in neuroblast clones are likely to reflect later-born mushroom-body neurons, which presumably inherit less Lis1 protein. Mushroom-body neurons born in early larval life undergo extensive reorganization of their dendritic projections during metamorphosis, such that the larval dendritic projections are completely pruned by 18 h after puparium formation, before the generation of adult dendrites[14] (see Fig. 2c). We therefore examined single-cell mushroom-body clones in adults, in which perdurance of Lis1 protein is less likely. *Lis1* dendrites were severely defective in several aspects (Fig. 5B, Table 1). In general, dendrites were much shorter in *Lis1* clones than in the wild type. The numbers of primary and higher-order branches, as well as overall branching complexity, were also greatly reduced (Table 1). At the end of the terminal branches, mushroom-body dendrites exhibited claw-like structures, probably representing a post-synaptic specialization (Fig. 5B, arrowheads in b). *Lis1*-mutant mushroom-body neurons also possessed such claws, although they were reduced in number and size (Fig. 5B, arrowheads in g). As these phenotypes were observed in single-labelled neurons, which were the only cells that were homozygous-mutant for *Lis1* in mosaic animals, these results demonstrate that Lis1 is cell-autonomously required for dendritic growth, branching and maturation.

Despite the defect in dendritic morphogenesis in *Lis1*-mutant neurons, pathfinding in *Lis1*-mutant axons was normal in both neuroblast clones and single-cell clones, at both the larval and adult stages (Figs 3c, d, 5A, c and 5B, f). Quantification of axonal branches in adult single-cell clones[15] also failed to reveal any significant differences between wild-type and *Lis1* neurons (numbers of major branches: wild-type, 1.78 ± 0.22; *Lis1*, 1.70 ± 0.15; numbers of minor branches: wild-type, 9.00 ± 0.62; *Lis1*, 8.30 ± 0.54; $n = 9$ (wild-type), 10 (*Lis1*); $P > 0.7$ and 0.4 for major and minor branch comparisons, respectively, as determined by t-test). These data indicate that Lis1 is preferentially required for growth and branching of dendrites, but not of axons.

Axonal-transport defects in *Lis1*-mutant neurons. Despite the normal pathfinding, axons of *Lis1*-mutant mushroom-body neurons in both neuroblast clones (Fig. 3c, d) and single-cell clones (Figs 5A, c, 5B, f and 6f; compare with Fig. 6e) at all stages examined exhibited swellings along the axonal path that were highly enriched for mCD8–GFP. These axonal swellings were very similar to the 'clogs' observed in mutants of motor proteins such as various subunits of kinesins (refs 16, 17; reviewed in ref. 18), indicating that Lis1 may be important in axonal transport.

mCD8–GFP is a transmembrane protein that is likely to be transported in vesicles for consititutive secretion. To investigate whether Lis1 is involved in other types of transport, we studied the distribution of other markers in *Lis1* neurons. We found that a synaptic-vesicle marker, n-synaptobrevin–GFP (n-syb–GFP)[19], which is likely to be transported by different motors to those that transport mCD8–GFP[18,20], also accumulates in large swellings along axons (Fig. 6b; compare with Fig. 6a). We also analysed the distribution of a Myc-epitope-tagged tubulin protein that we constructed (see Methods), as tubulin subunits are transported by yet another mechanism — slow axonal transport[18]. Myc–tubulin also accumulated in large swellings along axons (data not shown).

Mushroom-body neurons form synapses along the entire axon, as shown by the even distribution of n-syb–GFP at steady-state along the entire length of axons distal to the dendritic branching region (Fig. 6a; see also ref. 15). To exclude the possibility that the axon swellings we observed in *Lis1* mushroom-body neurons were abnormal synaptic specializations, we investigated marker distribution in photoreceptor axons in third-instar larvae, before entry to the brain lobes, at which time they should be devoid of synapses. We found analogous axonal swellings along the photoreceptor axons (Fig. 6c, d), which is consistent with the idea that Lis1 is important for axonal transport.

Dynein-heavy-chain mutants exhibit similar phenotypes to *Lis1*. Lis1 has been shown to be associated with microtubules[9], and the Lis1 homologue in *Aspergillus* has a strong genetic interaction with

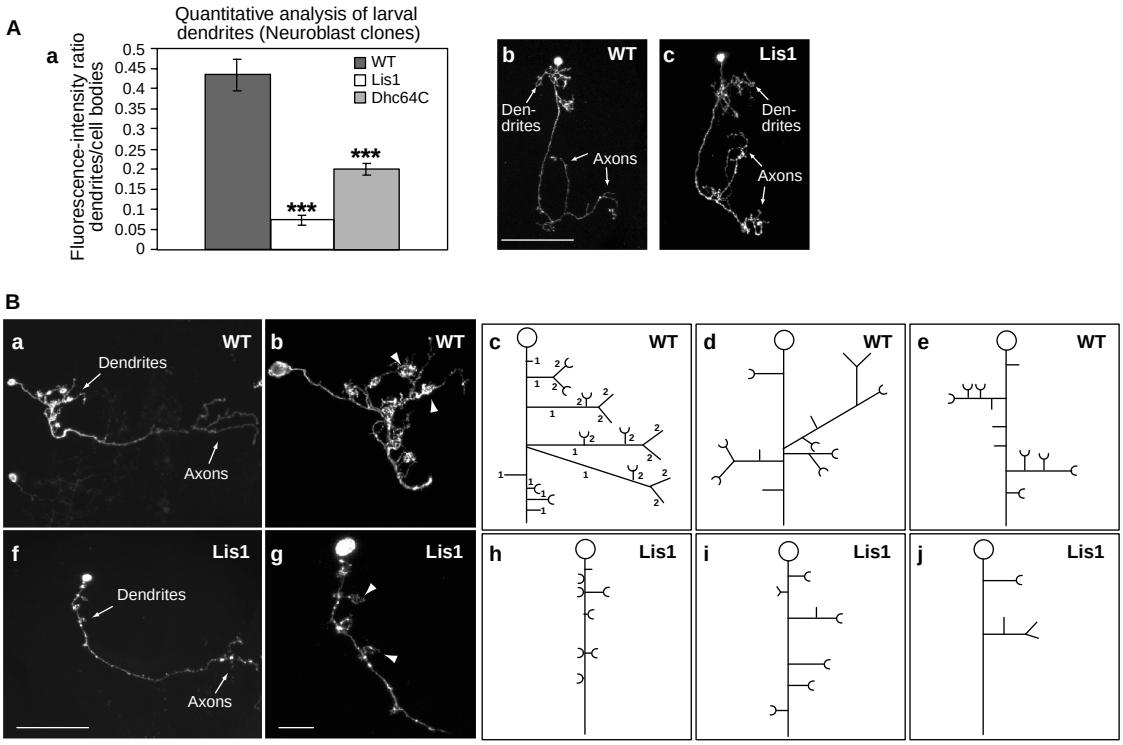

Figure 5 ***Lis1* is essential for dendritic morphogenesis of mushroom-body neurons. A**, Larval dendritic morphogenesis. **a**, Quantification of larval relative dendritic density of mushroom-body neuroblast clones (see Methods). Values are means ± s.e.m.; n = 10–13. The relative dendritic density is significantly reduced in *Lis1* and *Dhc64C* mutant clones (*t*-test, *** denotes $P < 0.001$). **b**, **c**, There is no obvious difference in dendritic complexity between wild-type (WT, **b**) and *Lis1* (**c**) single-cell clones at the larval stage. Scale bar represents 50 μm. **B**, Adult dendritic analysis. Wild-type (**a–e**) and *Lis1* (**f–j**) adult single-cell clones are compared as complete images (**a**, **f**), close-up views of the dendritic region (**b**, **g**; midline is situated to the right), schematic drawings of **b** and **g** (**c**, **h**), and two further representative drawings of each genotype (**d**, **e**, **i**, **j**). Note the marked difference in branch number and length between wild-type and *Lis1* clones, and that the terminal "claws" (arrowheads in **b** and **g** and indicated by half-circles in drawings) are generally much smaller in *Lis1* clones. Numbers in **c** indicate the branching order of dendrites (reversed Strahler method, see Methods). See Table 1 for quantification of adult dendrites. Scale bars represent 50 μm (**a**, **f**) and 10 μm (**b**, **g**). Genotypes of wild-type, *Lis1* and *Dhc64C* clones are as described in Fig. 3b, d and f, respectively.

Table 1 Quantative analysis of dendritic morphological parameters of adult single-cell mushroom-body clones

Genotype	Total no. segments	No. 1° branches	No. 2° branches	No. 3° branches	No. claws
[a]Wild-type (n = 16)	19.19 ± 0.98	6.94 ± 0.54	8.25 ± 0.66	1.00 ± 0.69	6.50 ± 0.45
[b]*Lis1* (n = 22)	6.59 ± 0.92	4.36 ± 0.62	2.05 ± 0.37	0	3.86 ± 0.40
[c]*Dhc64C* (n = 19)	8.26 ± 0.74	5.11 ± 0.43	2.79 ± 0.50	0	4.68 ± 0.47
[d]*Lis1*; *Dhc64C*/+ (n = 16)	6.00 ± 0.71	5.00 ± 0.52	0.88 ± 0.52	0	4.38 ± 0.45
[e]*Lis1*/+; *Dhc64C* (n = 11)	10.27 ±1.20	5.72 ±0.60	4.09 ± 0.69	0	5.55 ± 0.37

The total number of first-order segments, (1°) and second order (2°) branches, and of claws are significantly reduced in *Lis1* (b) and *Dhc64C* (c) mutants compared with wild-type (a) controls (one-tailed Student's *t* test, P<0.004 for all comparisons). Reducing one wild-type copy of *Dhc64C* (d) or *Lis1*(e) does not cause significant changes in the above parameters of *Lis1* and *Dhc64C* mutant clones (two-tailed Student's t-test, $p > 0.06$ for all comparisons).

Genotypes of a ,b and c are as in Fig. 3B, D and F, respectively. Other genotypes are as follows: d, *hs–FLP, UAS–mCD8/+; FRT^{G13}, Lis1$^{G10.14}$/FRT^{G13}, tubP–GAL80; FRT^{2A}, Dhc64C$^{4-19}$/+; GAL4^{OK107}/+*. e, *hs–FLP, UAS–mCD8/+; FRT^{G13}, Lis1$^{G10.14}$/+; FRT^{2A}, Dhc64C$^{4-19}$/FRT^{2A}, tubP–GAL80; GAL4^{OK107}/+*.

the cytoplasmic-dynein heavy chain[10]. We sought to test whether inactivation of dynein in the developing nervous system would have a similar phenotype to that of *Lis1* mutants. The best-studied cytoplasmic-dynein heavy chain in *Drosophila* is *Dhc64C* (refs 21, 22). Because cytoplasmic dynein functions in many cellular and developmental processes[22], we used the MARCM strategy (Fig. 2a, b) to generate marked mushroom-body clones that were homozygous for a strong loss-of-function mutation of *Dhc64C* (*Dhc64C$^{4-19}$*; refs 22, 23).

Like *Lis1* mutants, mushroom-body neuroblast clones homozygous for *Dhc64C* had a reduced clone size when examined in larvae (data not shown) and in adults (Fig. 3f). BrdU-labelling experiments showed a progressive reduction of BrdU incorporation at successive developmental stages (Fig. 4e). These results indicate

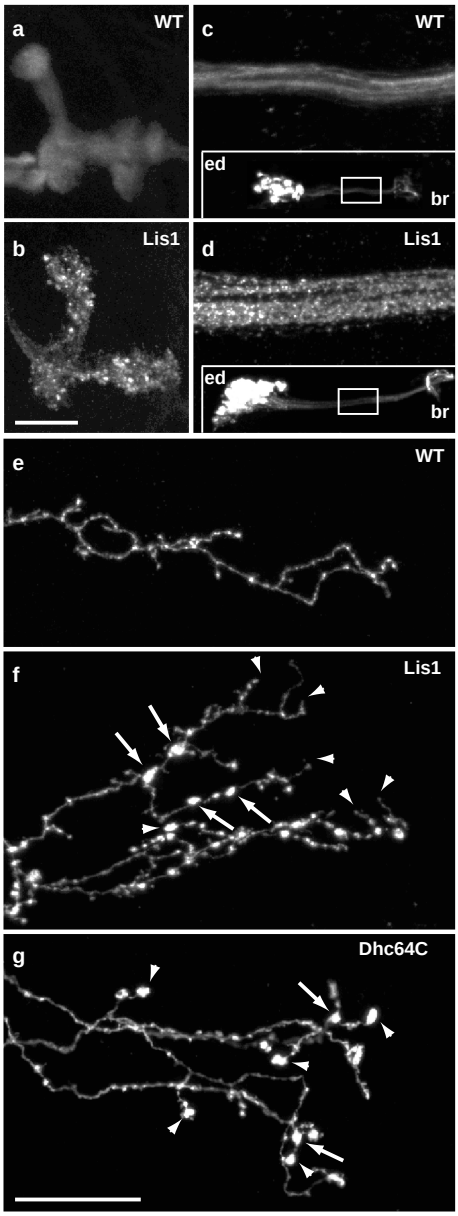

Figure 6 **Axonal swellings in *Lis1* and *Dhc64C* clones.** Two markers, UAS–n-syb–GFP (**a**, **b**) and UAS–mCD8–GFP (**c–g**) were used to visualize the larval mushroom-body axonal lobes (**a**, **b**) and photoreceptor axons (**c**, **d**; box in insets indicates where the enlarged images were taken from, eye disc (ed) is to the left and brain (br) is to the right). The γ-lobes of adult single-cell (**e**) or two-cell (**f**, **g**) clones of mushroom-bodies were viewed at higher magnification. Note the prominent axonal swellings in *Lis1* clones in different tissues (**b**, **d**, **f**), compared with the relatively even labelling of wild-type (WT) controls (**a**, **c**, **e**). In *Lis1* mushroom-body clones, swellings are distributed along the lengths of axons (**f**, arrows). In *Dhc64C* clones (**g**), although some swellings are found along the axons (arrows), they are preferentially located at axonal termini (arrowheads in **g**; compare with arrowheads in **f**). Scales are identical in **a** and **b** and in **c–g**; bars in **b** and **g** represent 50 μm and 10 μm, respectively. Genotypes are as follows: **a**, *GAL4^{C155}, hs–FLP/X or Y; FRT^{G13}/FRT^{G13}, tubP–GAL80; UAS–n-syb–GFP/+*. **b**, *GAL4^{C155}, hs–FLP/X or Y; FRT^{G13}, Lis1$^{G10.14}$/FRT^{G13}, tubP–GAL80; UAS–n-syb–GFP/+*. **c**, *GAL4^{C155}, hs–FLP, UAS–mCD8–GFP/X or Y; FRT^{G13}/FRT^{G13}, tubP–GAL80*. **d**, *GAL4^{C155}, hs–FLP, UAS–mCD8–GFP/X or Y; FRT^{G13}, Lis1$^{G10.14}$/FRT^{G13}, tubP–GAL80*. Genotypes in **e**, **f** and **g** are as described in Fig. 3b, d and f, respectively.

that *Dhc64C* clones may have a similar neuroblast-proliferation defect to that observed in *Lis1* clones, although this phenotype seems to be more variable in *Dhc64C*, possibly as a result of stronger perdurance of dynein heavy chain mRNA or protein. As in *Lis1*-mutant clones, we also found a significant reduction of dendritic complexity in *Dhc64C* neuroblast clones examined at the larval stage (Fig. 5a), although this effect was also less marked. Analysis of single-cell clones in adults also revealed a cell-autonomous requirement for *Dhc64C* in dendritic growth and branching, with a defect of similar extent to *Lis1* (Table 1). Lastly, axonal swellings were also characteristic of *Dhc64C* neuroblasts (Fig. 3f) and single- or two-cell clones (Fig. 6g) of mushroom-body neurons, as well as in photoreceptor axons (data not shown). Although axonal swellings in *Lis1* clones appeared along the entire axon, those in *Dhc64C* clones, although also found along the entire axon, seemed to preferentially decorate the ends of axonal branches (Figs 3f, 6g; compare with Fig. 6e, f). Assuming that, in these mushroom-body neurons, microtubule polarity is similar to vertebrate axons with plus ends orientated distally to soma[24], our observations provide strong genetic support that dynein is a retrograde motor for axonal transport.

To investigate possible genetic interactions between *Lis1* and *Dhc64C*, we carried out MARCM analysis of either *Lis1* or *Dhc64C* in animals heterozygous for the other gene (it is technically impossible to carry out double-homozygous mutant analysis using MARCM, because the two genes are on different chromosome arms). We used adult-dendrite morphogenesis for our analysis because it is readily quantifiable and the perdurance of Lis1 and dynein heavy chain is minimal. We detected no significant genetic interaction (Table 1, compare genotypes b and d, or c and e). This could mean that neither Lis1 nor *DHC64C* is dosage-sensitive, or alternatively, that the two genes work in the same genetic pathway, such that homozygous-null phenotypes of either component cannot be further modified by changing the dosage of the other component.

Discussion

Our genetic analysis has revealed striking similarities in the neuronal phenotypes of Lis1 and dynein-heavy-chain mutants (compare Fig. 3d and f). Similar defects in three different aspects of neuronal development and function were observed — neuroblast proliferation (Fig. 4e), dendritic elaboration (Table 1), and axonal transport (Fig. 6). Results from genetic-interaction studies are consistent with the idea that Lis1 and dynein function in the same pathway. It has recently been shown that Lis1 and dynein form a complex, and that overexpression of Lis1 in non-neuronal cells alters the distribution of the dynein complex and microtubule organization such that they mimic the properties of neurons[25]. Together, these findings indicate that Lis1 may work with cytoplasmic dynein to carry out much of its function in the nervous system.

In both *Lis1* and *Dhc64C* clones, neuroblast proliferation stops several days after clone generation. The simplest explanation for neuroblast-proliferation defects in *Lis1* and *Dhc64C* clones is the requirement of these proteins for cell-cycle progression. Indeed the essential function of dynein, and specifically of *Dhc64C*, in different steps of mitosis has been well documented (ref. 26 and references therein). The fact that Lis1 is required for both neuroblast proliferation and cell division in oogenesis[4] supports a general function of Lis1 in cell division. More detailed analyses are required to determine whether Lis1 and *Dhc64C* affect similar aspects of cell division.

Our genetic analysis have demonstrated that Lis1 and dynein are essential for dendritic morphogenesis. The effect of Lis1 on dendritic morphogenesis is striking. Single-cell mosaic analysis has revealed a marked reduction in dendritic length, branching complexity and terminal maturation (Fig. 5, Table 1). In contrast, Lis1 seems to be dispensible for axonal growth and targeting. One possible explanation for the differential requirement of Lis1 in dendritic compared with axonal development may relate to the

difference in microtubule organization in these two neuronal compartments. Experiments using mammalian pyramidal neurons have shown that microtubules in axons have all their plus ends pointing distally, whereas dendrites have microtubules in both orientations (reviewed in ref. 24). The same microtubule organization may also occur in *Drosophila* neurons. For instance, a fusion protein composed of a classical kinesin heavy chain and β-gal is specifically targeted to axonal termini[27], whereas a fusion protein between another microtubule motor Nod and β-gal is preferentially concentrated in dendrites in both sensory neurons[28] and mushroom-body neurons[15]. It is possible that 'minus-end-distal' microbutules in dendrites are particularly sensitive to perturbation of Lis1 or dynein activity, and that these microtubules are essential for elaboration or stabilization of dendrites. Another possible explanation of the differential effects in dendrites and axons is that dendritic structures may be more dynamic and undergo more post-developmental changes, and may therefore be more sensitive to genetic perturbation. In line with our findings, recent studies of the mouse hippocampus have revealed similar dendritic defects in heterotopic pyramidal neurons in *Lis1* heterozygotes[29]. Our single-cell mosaic analysis has further demonstrated that the requirement of Lis1 in dendritic morphogenesis is strictly cell-autonomous.

One of the most prominent features of *Lis1*-mutant neurons is the presence of axonal swellings. Several lines of evidence indicate that these may be caused by defects in axonal transport. First, these swellings appear to be identical to the axonal swellings previously reported as resulting from mutations in *Drosophila* classical kinesin heavy chain, light chain, dynein heavy chain, and the dynein-associated protein roadblock[16,17,30,31]. Axonal swellings in most of these other mutants have been shown by electron microscopy to correlate with the accumulation of cargo. We have carried out mosaic analyses of dynein and kinesin heavy chain in mushroom-body neurons, and found axonal swellings that were very similar to those in *Lis1*-mutant clones (Figs 3, 6, and data not shown). Second, these axonal swellings appear to become more severe as neurons grow older (as is apparent when comparing *Lis1* clones in larva with those in young adults, or those in young adults with those in old adults), which is consistent with the idea that such swellings are accumulations of cargo. Third, the swellings are unlikely to be a sign of neuronal degeneration or death because there is no obvious loss of *Lis1* neurons, as shown by comparing the sizes of neuroblast clones in young and old adults, or the frequency of single-cell clones in wild-type and *Lis1* mutants. Fourth, we have found analogous axonal swellings in *Lis1*-mutant photoreceptor axons (Fig. 6d) and sensory or motor axons outside the CNS (data not shown), which argues against the possibility that they are abnormal synaptic structures.

All of the markers we tested — a membrane marker, mCD8–GFP; a synaptic-vesicle marker, n-syb–GFP; and a slow-axonal-transport marker, Myc-tubulin — exhibited similar axonal swellings. This indicates either that Lis1 is required for all types of axonal transport, or that one type of axonal-transport defect causes a 'traffic jam', which indirectly affects all types of axonal transport[18]. It is worth noting that although *Lis1* and *Dhc64C* mutant neurons share the axonal-swelling phenotype, axonal swellings in *Dhc64C* appear to be preferentially located towards the termini of axonal branches. Such differences imply that the functions of Lis1 and dynein may not be identical in every aspect.

In summary, our genetic analyses have demonstrated pleiotropic functions of *Lis1* in neuroblast proliferation, dendritic elaboration and axonal transport. The fact that all of these processes involve the microtubule cytoskeleton, along with the similarity of *Lis1* and dynein-heavy-chain phenotypes in neurons, supports a general function of Lis1 in regulating the microtubule cytoskeleton. These new functions of Lis1, in addition to its documented role in neuronal migration, may contribute to the morphological and neurological phenotypes exhibited by lissencephalic patients. □

Methods

Fly culture and strains.

All flies were maintained at 25 °C on standard medium. The following strains were generated using standard genetic methods and were used in this study: 1, *GAL4^{C155}, hs–FLP, mCD8–GFP; FRT^{G13}, tubP–GAL80*. 2, *hs–FLP, mCD8–GFP; FRT^{G13}, tubP–GAL80/CyO; GAL4^{OK107}*. 3, *GAL4^{C155}, hs–FLP, mCD8–GFP; FRT^{2A}, tubP–GAL80/TM3*. 4, *hs–FLP, mCD8–GFP; FRT^{2A}, tubP-GAL80/TM3; GAL4^{OK107}*. 5, *FRT^{G13}, Lis1$^{G10.14}$/CyO, UAS–n-syb–GFP*. 6, *FRT^{G13}, Lis1$^{G10.14}$/CyO; FRT^{2A}, Dhc64C$^{4–19}$/TM6*. *FRT^{2A}, Dhc64c$^{4–19}$/TM6* (ref. 23) was provided by T. Hays. All other stocks used in this study have been previously described[4,13,15]. GAL4^{OK107} (ref. 14) was used as the driver to visualize mushroom-body clones in most situations; GAL4^{C155} (ref. 13) was used for clones of photoreceptor cells and segmental nerves. Unles otherwise stated, mCD8–GFP (ref. 13) was used as the marker.

New transgenic lines.

UAS–Lis1: Lis1 complementary DNA (pZL701; ref. 4) was subcloned into UAS-CaSpeR vector pUAST using *Not*I and *Xho*I as restriction sites to generate UAS–Lis1 (pZL1043). UAS–HA–Lis1: an HA fragment was amplified by polymerase chain reaction (PCR) and subcloned into Lis1 cDNA (pZL832) using an *Nde*I site, which was created by site-directed mutagenesis at the start codon of Lis1 cDNA, to generate UAS–HA–Lis1 (pZL1078). UAS–Myc–α1tub: the open reading frame (ORF) of α1tub, from the second codon to the stop codon, was PCR-amplified on a genomic α1tub construct[32] (provided by W. E. Theurkauf), and subcloned using *Eco*RI and *Bgl*II sites into pβ-2Xmyc-B to create a new ORF of Myc–α1tub (pZL1080), which was then subcloned into pUAST using *Not*I and *Kpn*I as restriction sites to generate UAS–Myc–α1tub (pZL1082). All constructs were injected into *y w* strain to generate transgenic flies according to standard procedures[33].

Whole-mount *in situ* tissue hybridization.

In situ hybridization to whole-mount embryos was carried out as described[4].

Mosaic analysis with a repressible cell marker (MARCM), immunohistochemistry, and microscopy.

Eggs (0–5 h old) from appropriate crosses (for genotypes, see figure and table legends) were collected on standard food and aged at 25 °C. A 50-min heat shock at 37 °C was applied 4 h, 19 h or 2 days later, for induction of clones from segmental nerves, mushroom-bodies or photoreceptor cells, respectively. At the desired stages (late-third-instar larva or adult), brains were dissected, fixed, and stained as described[13]. All samples were antibody-stained, except that for dendritic quantification of neuroblast clones, in which GFP fluorescence was used. Primary antibody dilutions were as follows: mouse monoclonal anti-HA (Babco, Richmond, California), 1:1000; rat monoclonal anti-mCD8 α-subunit (Caltag, Burlingame, California), 1:100; rat monoclonal anti-BrdU (Harlan sera-lab, Indianapolis, Indiana), 1:250; mouse monoclonal anti-Myc (Santa Cruz), 1:50; mouse monoclonal anti-GFP (Quantum, Carlsbad, California), 1:200; rabbit anti-lamin (P. Fisher, SUNY, Stony Brook, New York), 1:50. Cy3-conjugated secondary antibody was used at a 1:500 dilution. For nuclear staining, samples were treated with RNase A (Sigma) at 400 μg ml^{-1} for 2 h and incubated with propidium iodide (Sigma) at 10 μg ml^{-1} for 20 min. Images were obtained with a Bio-Rad MRC 1024 laser-scanning confocal microscope, using the Laser Sharp image-collection program. Images were processed using Adobe Photoshop.

BrdU-incorporation experiment.

Larvae were heat-shocked 0–2 h after hatching. At the time of the BrdU pulse, larvae were transferred to standard food containing 0.7 mg ml^{-1} BrdU for 3 h, and then returned to standard medium until dissection at the late-third-instar stage. A 30-min incubation in 2 N HCl/PBS was included before BrdU staining.

Quantification of dendritic and axonal morphology.

Relative dendrite densities of larval mushroom-body clones were quantified as described[15]. Adult single-cell dendritic branches were traced through each confocal plane and ordered by the reversed Strahler method[34]. In this method, all terminal segments are designated as 'first-order'. A second-order branch is formed where two first-order segments join. To reverse, the highest Strahler order is designated as first-order and all other orders are consecutively assigned orders two, three, etc. The number of dendritic segments was derived by counting the number of dendrite branching points and dendrite terminal ends. For axons, branches longer than one-quarter of the lobe length were defined as major branches, and all others as minor branches.

RECEIVED 18 MAY 2000; REVISED 30 JUNE 2000; ACCEPTED 17 JULY 2000;
PUBLISHED 29 SEPTEMBER 2000.

1. Dobyns, W. B., Reiner, O., Carrozzo, R. & Ledbetter, D. H. Lissencephaly. A human brain malformation associated with deletion of the LIS1 gene located at chromosome 17p13. *J. Am. Med. Assoc.* **270,** 2838–2842 (1993).
2. Reiner, O. *et al.* Isolation of a Miller–Dieker lissencephaly gene containing G protein β-subunit-like repeats. *Nature* **364,** 717–721 (1993).
3. Hirotsune, S. *et al.* Graded reduction of Pafah1b1 (Lis1) activity results in neuronal migration defects and early embryonic lethality. *Nature Genet.* **19,** 333–339 (1998).
4. Liu, Z., Xie, T. & Steward, R. Lis1, the *Drosophila* homolog of a human lissencephaly disease gene, is required for germline cell division and oocyte differentiation. *Development* **126,** 4477–4488 (1999).
5. Swan, A., Nguyen, T. & Suter, B. *Drosophila* Lissencephaly-1 functions with Bic-D and dynein in oocyte determination and nuclear positioning. *Nature Cell Biol.* **1,** 444–449 (1999).
6. Xiang, X., Osmani, A. H., Osmani, S. A., Xin, M. & Morris, N. R. NudF, a nuclear migration gene in *Aspergillus nidulans*, is similar to the human LIS-1 gene required for neuronal migration. *Mol. Biol. Cell* **6,** 297–310 (1995).
7. Neer, E. J., Schmidt, C. J., Nambudripad, R. & Smith, T. F. The ancient regulatory protein family of WD-repeat proteins. *Nature* **371,** 297–300 (1994).
8. Hattori, M., Adachi, H., Tsujimoto, M., Arai, H. & Inoue, K. Miller–Dieker lissencephaly gene encodes a subunit of brain platelet-activating factor. *Nature* **370,** 216–218 (1994).

9. Sapir, T., Elbaum, M. & Reiner, O. Reduction of microtubule catastrophe events by LIS1, platelet-activating factor acetylhydrolase subunit. *EMBO J.* **16,** 6977–6984 (1997).
10. Willins, D. A., Liu, B., Xiang, X. & Morris, N. R. Mutations in the heavy chain of cytoplasmic dynein suppress the nudF nuclear migration mutation of *Aspergillus nidulans. Mol. Gen. Genet.* **255,** 194–200 (1997).
11. Willins, D. A., Xiang, X. & Morris, N. R. An alpha tubulin mutation suppresses nuclear migration mutations in *Aspergillus nidulans. Genetics* **141,** 1287–1298 (1995).
12. Brand, A. H. & Perrimon, N. Targeted gene expression as a means of altering cell fates and generating dominant phenotypes. *Development* **118,** 401–415 (1993).
13. Lee, T. & Luo, L. Mosaic analysis with a repressible cell marker for studies of gene function in neuronal morphogenesis. *Neuron* **22,** 451–461 (1999).
14. Lee, T., Lee, A. & Luo, L. Development of the *Drosophila* mushroom bodies: sequential generation of three distinct types of neurons from a neuroblast. *Development* **126,** 4065–4076 (1999).
15. Lee, T., Winter, C., Marticke, S. S., Lee, A. & Luo, L. Essential roles of *Drosophila* RhoA in the regulation of neuroblast proliferation and dendritic but not axonal morphogenesis. *Neuron* **25,** 307–316 (2000).
16. Hurd, D. D. & Saxton, W. M. Kinesin mutations cause motor neuron disease phenotypes by disrupting fast axonal transport in *Drosophila. Genetics* **144,** 1075–1085 (1996).
17. Gindhart, J. G. Jr, Desai, C. J., Beushausen, S., Zinn, K. & Goldstein, L. S. B. Kinesin light chains are essential for axonal transport in *Drosophila. J. Cell Biol.* **141,** 443–454 (1998).
18. Goldstein, L. S. B. & Yang, Z. Microtubule-based transport systems in neurons: the roles of kinesins and dyneins. *Ann. Rev. Neurosci.* 23, 39–71 (2000).
19. Ito, K. *et al.* The organization of extrinsic neurons and their implications in the functional roles of the mushroom bodies in *Drosophila melanogaster* meigen. *Learning and Memory* **5,** 52–77 (1998).
20. Okada, Y., Yamazaki, H., Sekine-Aizawa, Y. & Hirokawa, N. The neuron-specific superfamily protein KIF1A is a unique monomeric motor for anterograde axonal transport of synaptic vesicle precursors. *Cell* **81,** 769–780 (1995).
21. Li, M-g., McGrail, M., Serr, M. & Hays, T. S. *Drosophila* cytoplasmic dynein, a microtubule motor that is asymmetrically localized in the oocyte. *J. Cell Biol.* **126,** 1475–1494 (1994).
22. Gepner, J. *et al.* Cytoplasmic dynein function is essential in *Drosophila melanogaster. Genetics* **142,** 865–878 (1996).
23. McGrail, M. & Hays, T. S. The microtubule motor cytoplasmic dynein is required for spindle orientation during germline cell divisions and oocyte differentiation in *Drosophila. Development* **124,** 2409–2419 (1997).
24. Baas, P. W. Microtubules and neuronal polarity: lessons from mitosis. *Neuron* **22,** 23–31 (1999).
25. Smith, D. S. *et al.* Regulation of cytoplasmic dynein behaviour and microtubule organization by mammalian Lis1. *Nature Cell Biol.* **2,** 767–775 (2000).
26. Robinson, J. T., Wojcik, E. J., Sanders, M. A., McGrail, M. & Hays, T. S. Cytoplasmic dynein is required for the nuclear attachment and migration of centrosomes during mitosis in *Drosophila. J. Cell Biol.* **146,** 597–608 (1999).
27. Giniger, E., Wells, W., Jan, L. Y. & Jan, Y. N. Tracing neurons with a kinesin-·-galactosidase fusion protein. *Roux's Arch. Dev. Biol.* **202,** 112–122 (1993).
28. Clark, I. E., Jan, L. Y. & Jan, Y. N. Reciprocal localization of Nod and kinesin fusion proteins indicates microtubule polarity in the *Drosophila* oocyte, epithelium, neuron and muscle. *Development* **124,** 461–470 (1997).
29. Fleck, M. W. *et al.* Hippocampal abnormalities and enhanced excitibility in a murine model of human lissencephaly. *J. Neurosci.* **20,** 2439–2450 (2000).
30. Bowman, A. B. *et al. Drosophila* roadblock and Chlamydomonas LC7: a conserved family of dynein-associated proteins involved in axonal transport, flagellar motility, and mitosis. *J. Cell Biol.* **146,** 165–179 (1999).
31. Martin, M. A. *et al.* Cytoplasmic dynein, the dynactin complex and kinesin are interdependent and essential for fast axonal transport. *Mol. Biol. Cell* **10,** 3717–3728 (1999).
32. Theurkauf, W. E., Baum, H., Bo, J. & Wensink, P. C. Tissue-specific and constitutive a-tubulin genes of *Drosophila melangaster* code for structurally distinct proteins. *Proc. Natl Acad. Sci. USA* **83,** 8477–8481 (1986).
33. Spradling, A. C. & Rubin, G. M. Transposition of cloned P elements into *Drosophila* germ line chromosomes. *Science* **218,** 341–347 (1982).
34. Berry, M. & Bradley, P. The growth of the dendritic trees of Purkinje cells in the cerebellum of the rat. *Brain Res.* **112,** 1–35 (1976).

ACKNOWLEDGEMENTS

We thank T. Hays and W. E. Theurkauf for reagents, L-H. Tsai for sharing results before publication, and R. Kopito and members of the Luo laboratory for discussions and comments on the manuscript. Z.L. is a fellow of the Epilepsy Training Grant from Stanford University. This work was supported by NIH grant R01-NS36623 and fellowships from the McKnight, Klingenstein and Sloan foundations to L.L.

Correspondence and requests for materials should be addressed to L.L.